

HIGH STRAIN FRACTURE ANALYSIS

C. K. Tsai*, H. W. Shen*, X. X. Chen*,
L. G. Luo* and M. Z. Zheng**

*Central Iron and Steel Research Institute,
Beijing, China

**Aircraft Strength Research Institute, Xian, China

ABSTRACT

High strain fracture analysis deals with the growth of a small crack within a large zone of high loading strain which may be monotonic, cyclic or time-dependent creeping. In this paper COD and J integral analysis and experimental calibration for high strain crack problems are given and compared. Attention has been drawn to the difference between general yielding and ligament yielding, and especially on the ligament yielding disturbance in the experimental calibration of COD and J-integral for high strain fracture analysis. The applicability and limitations of the analysis in predicting the fracture and life of specimens and engineering components with the small pre-existing crack in the region of high nominal strain under monotonic, cyclic or time-dependent creeping condition are discussed.

KEYWORDS

Elastic-plastic fracture mechanics; crack growth; J-integral; crack opening displacement; ligament yielding; general yielding; stress rupture; strain fatigue; crack tolerance analysis.

INTRODUCTION

A series of fractures involve the growth of a small crack within a large zone of high loading strain which may be monotonic, cyclic or time-dependent creeping. This type of fracture may be denominated by "high strain fracture" and is often met in brittle fracture of pressure vessels and other welding structure, as well as in low cycle strain fatigue and creep fracture of machine components where growth of small pre-existing crack within large strain-cycling or creeping

zone may significantly reduce the strength and life of the components. However, in contrast to the extensive investigation on specimens with deep crack where ligament yielding occurs, relatively little attention has been paid to general yielding specimens in which a small crack is fully encompassed by large zone of gross yield expanding all over the whole specimen. In this paper, high strain crack problems are reviewed using the formulations for pure power hardening model, COD and J-integral formulas of small crack within area of high nominal strain for elastic-plastic materials are discussed and compared with the results of experimental calibration. The above analytical and calibrating results are then used for analysing crack growth rate and life of specimens with small pre-existing crack under plastic fatigue and creep condition.

FORMULATION OF HIGH STRAIN CRACK PROBLEMS

High strain crack problems are best formulated by using the incompressible, pure power hardening model (Goldman and Hutchinson, 1975; Shih and Hutchinson, 1976) with stress-strain relationship

$$\varepsilon = \alpha \sigma^n \quad (1)$$

in simple tension and its generalization

$$\varepsilon_{ij} = \frac{3}{2} \alpha \sigma_e^{n-1} \cdot S_{ij} \quad (2)$$

for complex stress-strain state.

If boundary value problems based on (2) are considered where the components of all the boundary stress vectors are proportional to a common load parameter, then as first shown by Ilyushin (1946) and discussed recently by Goldman and Hutchinson (1975) and by Tsai and his coworkers (1977, 1978), the stress at each point in the body also varies linearly with the load parameter and the functional form of the stress-strain field solutions is extremely simple and suitable for elastic plastic fracture mechanical analysis. Thus, for center crack specimen of width $2b$, crack length $2a$, loaded by uniform stress remote from the crack, the functional form of the solution is

$$\sigma_{ij} = \sigma \cdot \hat{\sigma}_{ij}(\bar{x}/a, a/b, n) \quad (3)$$

$$\varepsilon_{ij} = \alpha \sigma^n \cdot \hat{\varepsilon}_{ij}(\bar{x}/a, a/b, n) \quad (4)$$

$$u_i/a = \alpha \sigma^n \cdot \hat{u}_i(\bar{x}/a, a/b, n) \quad (5)$$

Furthermore, COD and J-integral can be expressed as

$$\delta = (\alpha \sigma^n) a \cdot \hat{\delta}(a/b, n) \quad (6)$$

$$J = a(\alpha \sigma^{n+1}) \hat{J}(a/b, n) \quad (7)$$

where $\delta = u_2(0,0^+) - u_2(0,0^-)$ is the crack opening displacement at the center of the crack, but it has been shown in Goldman's paper (1975), for engineering materials of common occurrence with $n \geq 5$, the COD at the center of the crack is a good approximation to the near-tip COD. The dimensionless functions $\hat{\delta}(a/b, n)$ and $\hat{J}(a/b, n)$ are dependent only upon the nondimensionalized geometrical parameter a/b and the material parameter n , but independent of the stress σ . They had been calculated by F.E. method for various a/b and n . However, in order to convert these F.E. results into simple analytic expressions convenient for engineering use and to obtain the formulas for small crack within areas of high nominal strain by extrapolation, two significantly different types of yielding or distribution of strains due to the different geometric condition (values of a/b) of the specimens should be recognized. Figure 1 shows the different schemes of strain distribution under two different geometric conditions.

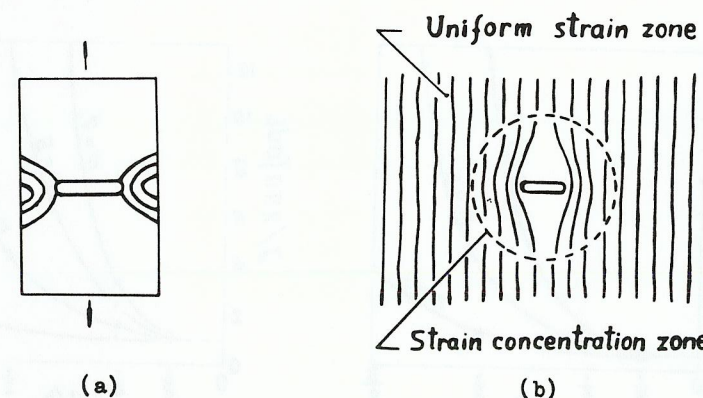


Fig. 1. Two typical full yielding schemes for tension plate. (a) Ligament yielding. (b) General yielding.

In the case of narrow ligament, due to the fact that the net section stress at the ligament $\sigma_{net} = b\sigma/(b-a)$ is apparently greater than the uniform stress σ remote from the crack, the strain concentration zone will be located mainly in the ligament, thus we call it ligament yielding case. In the case of a crack in an infinitely wide plate ($a/b \rightarrow 0$), due to the absence of the two side boundaries of the specimen, the strain concentration zones of the crack will entirely be enveloped by a general yielding zone of uniform strain remote from the crack. This type of yielding is denominated by "general yielding" in the present paper.

The difference in the expressions of COD and J-integral due to the difference in the distribution of strains should be found in the expression of $\hat{\delta}(a/b, n)$ and $\hat{J}(a/b, n)$ in equations (6) and (7). Thus, in general yielding case as happens in the infinitely wide plate, $a/b \rightarrow 0$, $\hat{\delta}$ will be only dependent upon n and the expression (6) can be rewritten in the type of Wells' formula (note that $\epsilon = \alpha \sigma^n$):

$$\delta = 2\pi q a \epsilon \tag{8}$$

where the shape factor of the crack specimen q is defined by $q = \hat{\delta}(n)/2\pi$ and is only dependent upon the material parameter n . However, in the case of strain concentration in the ligament, $q = \hat{\delta}(a/b, n)/2\pi$ will vary strongly with the variation of the ratio a/b . Figure 2(a) shows the results of F.E. calculation of the COD for center cracked plate made of pure power hardening materials in the state of plane strain. It is apparent that when $a/b \rightarrow 0$, for engineering materials of common occurrence with $n=5-7$, $\delta/2\pi a \epsilon = q \rightarrow 1$ is a good engineering approximation for pure power hardening material under general yielding condition.

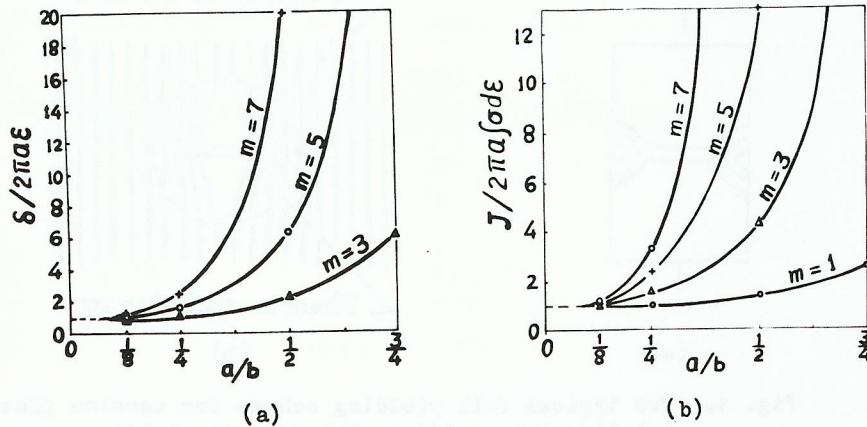


Fig. 2. Extrapolation of plane strain F.E. results to $a/b \rightarrow 0$ to obtain the shape factor q and Q for general yielding.

By interpolation of the small scale yielding solution and the above fully plastic solution, simple estimates of COD for elastic plastic materials under general yielding condition can be obtained. Thus, COD of a through thickness crack of length $2a$ in an infinitely wide plate under small scale yielding condition is given by DBCS-model:

$$\delta_{el} = \frac{8\bar{\sigma}a}{\pi E} \ln \sec\left(\frac{\pi\sigma}{2\bar{\sigma}}\right) = \frac{8a\epsilon_0(\bar{\sigma})}{\pi} \ln \sec\left(\frac{\sigma_0 \cdot \pi \epsilon_{el}}{2\bar{\sigma}\epsilon_0}\right) \tag{9}$$

where the yield stress σ_0 has been replaced by flow stress $\bar{\sigma}$ to account for the stress elevation within the yielding zone by strain hardening and triaxiality, and $\epsilon_0 = \sigma_0/E$, $\epsilon_{el} = \sigma/E$.

On the other hand, the fully plastic contribution of COD, δ_p , under general yielding condition is given by the above result for pure power hardening materials (with $n=5-7$, $q=1$)

$$\delta_p = 2\pi a \epsilon_p \tag{10}$$

To interpolate over the entire range of yielding, we may take the sum of the small scale yielding contribution δ_{el} and the fully plastic contribution δ_p , i.e. $\delta = \delta_{el} + \delta_p$, then we have (note that $\epsilon_p = \epsilon - \epsilon_{el}$),

$$\phi \equiv \frac{\delta}{2\pi a \epsilon_0} = \frac{\epsilon}{\epsilon_0} - \left[\frac{\epsilon_{el}}{\epsilon_0} - \frac{4}{\pi^2} \left(\frac{\bar{\sigma}}{\sigma_0}\right) \ln \sec\left(\frac{\sigma_0 \cdot \pi \epsilon_{el}}{2\bar{\sigma}\epsilon_0}\right) \right] \tag{11}$$

As the general yielding is not too deep, we may put $\epsilon_{el}/\epsilon_0 \approx 1$ and $\bar{\sigma}/\sigma_0 = 1.15$, then the Burdekin relation results:

$$\phi = \frac{\epsilon}{\epsilon_0} - 0.25 \tag{12}$$

The above interpolating result for general yielding case is valid only when no ligament yielding disturbance is present. However, in most wide plate test condition, ligament yielding is hardly avoidable due to insufficient smallness of the crack length to plate width ratio a/b , or due to the presence of broad yielding plateau which implies nonhardening or perfect plasticity with $n \rightarrow \infty$. In this mixed-mode yielding case, the measured $\phi - \epsilon/\epsilon_0$ curve demonstrates clearly four stages of deformation as shown in Fig. 3 (Sato and Toyoda, 1979; Tsai and coworkers, 1978):

1. The small scale yielding stage.
2. The ligament yielding stage. In this stage, in terms of the nominal strain ϵ measured within the gauge $2y$, the nondimensional COD of the center cracked strip can be expressed as

$$\phi \equiv \frac{\delta}{2\pi a \epsilon_0} = \frac{1}{\pi} \left(\frac{y}{a}\right) \frac{\epsilon}{\epsilon_0} + A \tag{13}$$

and the slope of the $\phi - \epsilon/\epsilon_0$ curve is $d\phi/d(\epsilon/\epsilon_0) = y/\pi a$. Due to the variation of the gauge length to crack length ratio y/a , the measured curve $\phi - \epsilon/\epsilon_0$ may locate above the Burdekin design curve when $y/\pi a > 1$, as shown in Fig. 3, or below the design curve when $y/\pi a < 1$. Thus, the scattering of the wide plate testing curves ($\phi - \epsilon/\epsilon_0$) above or below the design curve can be explained as due to the disturbance of ligament yielding with different gauge length to crack length ratio a/y .

3. The stage of spreading of the Lüders band or the initial yielding (corresponding to the yield plateau) in the remaining parts of the plate with COD and ligament zone frozen.
4. The general yielding stage in the whole plate with power hardening. The slope of the curve $\phi - \epsilon/\epsilon_0$ in this stage is $d\phi/d(\epsilon/\epsilon_0) = 1$ for center cracked strip as predicted by equation (10) and (11).

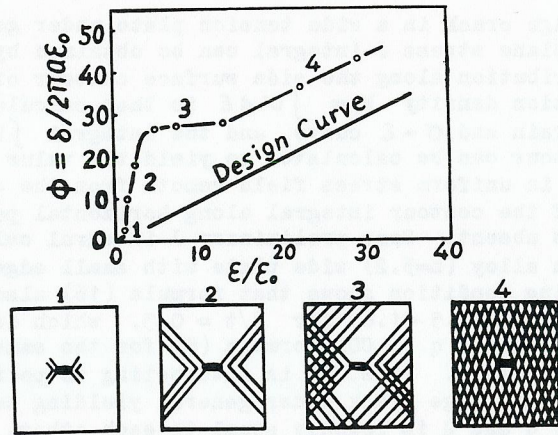


Fig. 3. Due to the ligament yielding disturbance and presence of yielding plateau four stages of deformation are present in wide plate test: 1. Small scale yielding. 2. Ligament yielding. 3. Spreading of Lüders band. 4. General yielding.

In actual engineering components surface crack is usually met. Theoretically, equation (8) also holds for surface crack in a semi-infinite body of pure power hardening material, except that the shape factor q should be dependent upon $a/2c$, and similarly, for surface crack in a semi-infinite body of elastic-plastic material under general yielding condition:

$$\phi = q \left(\frac{\epsilon}{\epsilon_0} - 0.25 \right) \quad (14)$$

Since no F.E. calculation has been done for surface crack under general yielding condition, the applicability of the formula (14) and the shape factor q can only be determined by experimental calibration. Figure 4 shows some result of experimental calibration on wide plates containing surface crack of various $a/2c$ and a/t . The measured $\phi \sim \epsilon/\epsilon_0$

curve agrees well with the formula (14) only when $a/t \leq 1/10$ with $q=0.75$ for surface crack of $a/2c=0.11$, in which local ligament yielding stage, that is, local yielding at the remaining ligament ($t-a$) behind the crack is essentially absent. For the other two specimens with large a/t , the local ligament yielding stage precedes the general yielding stage and makes the $\phi \sim \epsilon/\epsilon_0$ curve to go high above the Burdekin's design curve owing to the large gauge length to crack depth ratio y/a .

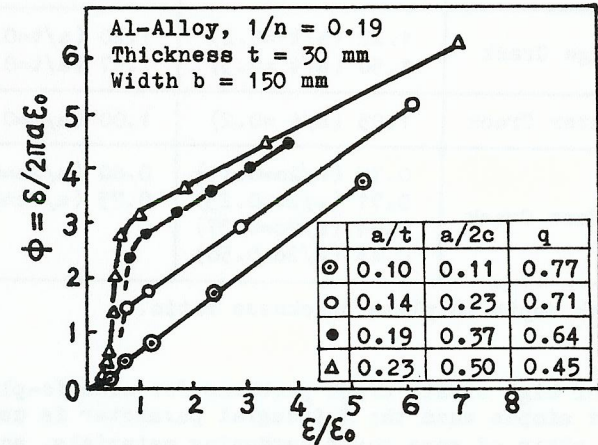


Fig. 4. Measured $\phi - \epsilon/\epsilon_0$ curve and shape factor q for wide plate with small surface crack of different geometry.

According to the extrapolating result of F.E. calculations given by Shih and Hutchinson (1976), for center crack in an infinite sheet under plane stress state,

$$\delta = [3.85 \sqrt{n} (1 - 1/n) + 4/n] \alpha a \sigma^n \quad (15)$$

and the shape factor in eq. (8) and (14) should be

$$q = [3.85 n (1 - 1/n) + 4/n] / 2\pi$$

which is somewhat larger than unity for $n > 5$. However, for small surface or edge crack within large general yielding zone of engineering components where crack depth to thickness (or section size) ratio is small, the stress state at the crack tip region is plane strain, whereas it is plane stress remote from the crack. The shape factor q may have the value between the F.E. results of the two stress states. Thus, it is valuable to conduct experimental calibration of COD versus ϵ/ϵ_0 under general yielding condition to obtain the actual shape factor q for various materials and crack geometry. Some experimental re-

sults of the shape factor q for center crack, edge crack and surface crack of various $a/2c$ under general yielding condition are listed in Table 1.

TABLE 1 Measured Shape Factor q for General Yielding

	Aluminium Alloy $1/n = 0.19$	C/Mn Steel $1/n = 0.24$
Edge Crack	1.20 ($a/t^*=0.2$) 1.50 ($a/t = 0.3$)	1.20 ($a/t=0.2$) 1.57 ($a/t=0.4$)
Center Crack	1.05 ($a/t = 0.2$)	1.00 ($a/t=0.5$)
Surface Crack	0.77 ($a/2c=0.11$) 0.71 ($a/2c=0.23$) 0.64 ($a/2c=0.37$) 0.45 ($a/2c=0.50$)	0.80 ($a/2c=0.2$) 0.75 ($a/2c=0.4$)

*Crack depth to plate thickness ratio.

Formulation of high strain crack problems for elastic-plastic materials is most simple when the J -integral parameter is used. Thus, for center crack strip of pure power hardening materials, equation (7) can be rewritten as

$$J = 2\pi Qa \int \sigma d\varepsilon \quad (16)$$

where $\int \sigma d\varepsilon = \alpha \left(\frac{n}{n+1} \right) \left(\frac{\sqrt{3}}{2} \sigma \right)^{n+1}$ and $Q = \hat{J}(a/b, n) / [2\pi \left(\frac{n}{n+1} \right) \left(\frac{\sqrt{3}}{2} \right)^{n+1}]$

for plane strain. Using the F.E. results of plane strain J -integral for center crack strips of pure power hardening material calculated by Goldman and Hutchinson (1975), curves of $J/2\pi a \int \sigma d\varepsilon$ versus a/b are plotted in Fig. 2(b) for different values of n . Extrapolation to $a/b \rightarrow 0$ for infinite wide plate shows that at least for $n=1-7$, the shape factor $Q = J/2\pi a \int \sigma d\varepsilon \rightarrow 1$ may serve a good engineering approximation for general yielding case.

Since equation (16) is valid not only for fully plastic material but also for linear elastic material in which $\int \sigma d\varepsilon = \sigma^2/2E'$ and $J = \pi a \sigma^2/E'$, formula for estimating the J -integral of elastic-plastic materials over the entire range of loading can readily be obtained by taking the sum of the linear elastic contribution

$J_{el} = 2\pi Qa \int \sigma d\varepsilon_{el}$ and the fully plastic contribution

$J_p = 2\pi Qa \int \sigma d\varepsilon_p$ The same equation (16) results with $J=J_{el}+J_p$ and $d\varepsilon = d\varepsilon_{el} + d\varepsilon_p$. Thus, the simple formula (16) is applicable

also for elastic-plastic material over the entire range of general yielding.

Comparing formula (16) with the plane stress J -integral formula for infinite wide plate obtained by Shih and Hutchinson (1976)

$$J = \alpha [3.85 n(1-1/n) + \pi/n] a \sigma^{n+1} \quad (17)$$

we have $Q = [3.85 n(1-1/n) + \pi/n] \cdot [(n+1)/2\pi n]$, which is somewhat larger than unity for $n=5-7$.

For small edge crack in a wide tension plate under general yielding condition, plane stress J -integral can be obtained by measuring the strain distribution along the side surface contour of the specimen. The deformation density $W = \int \sigma d\varepsilon$ is then calculated using the measured strain and $\sigma - \varepsilon$ curve, and the integral $\int W dy$ along side surface contour can be calculated to yield the value of J -integral, since there is uniform stress field remote from the crack, the contribution of the contour integral along horizontal path remote from the crack is absent. Some preliminary J -integral calibration results on aluminium alloy ($n=5.2$) wide plate with small edge crack under general yielding condition shows that formula (16) also holds with the shape factor $Q = 1.5 \sim 1.6$ for $a/t = 0.3$, which is roughly equal to the shape factor q in COD formula (8) for the same crack geometry as shown in Table 1. Thus, it is interesting to point out that for center crack and edge crack under general yielding condition the two shape factor q and Q is roughly equal to each other.

Finally, although the two-dimensional of J -integral is meaningless for surface crack, we can nevertheless define an applied or equivalent J -parameter by the following expression

$$J \equiv \left(\frac{n}{n+1} \right) \sigma \delta \quad (18)$$

which appears to be a good approximation in two-dimensional case for pure power hardening materials under general yielding condition and can be obtained by comparing equations (15) and (17). For surface crack, the physical meaning of the definition (18) may be interpreted as follows. Along the crack border segment which is large compared with the COD value, the near-tip field changes negligibly and is essentially two-dimensional, the relationship (18) has its usual physical meaning that the defined J parameter determines the strength of the crack tip singularity. Substituting (8) and (1) into (18), we arrive at the following expression

$$J \equiv \left(\frac{n}{n+1} \right) \sigma \delta = 2\pi qa \int \sigma d\varepsilon \quad (19)$$

for the equivalent J parameter which determines the amplitude of the HRR singularity at the segment of the crack border where the crack

opening displacement δ , the crack depth a , and so the shape factor q for the surface crack are measured. It is easy to show that formula (19) is a good approximation also for elastic plastic material over the entire range of general yielding with $d\varepsilon = d\varepsilon_{el} + d\varepsilon_p$. Thus, the simple J parameter formula (19) can be used for analysing the growth of a surface crack provided the shape factor q is obtained by experimental COD calibration as listed in Table 1.

CRACK TOLERANCE WITHIN AREA OF HIGH STRAIN

Critical crack-size analysis in areas of high nominal strain is a practically important task for the prevention of brittle fracture in pressure vessels and other welding structures. Before applying the fracture criterion $\delta = \delta_c$ to the evaluation of critical crack size, it is necessary to establish the functional relationship between the crack opening displacement δ , the crack size and the nominal strain. The relation usually employed is Wells' and Burdekin's formulas (Wells, 1963; Burdekin, 1971), which are empirical formulas deduced from wide plate experimental data. However, as had been discussed above, wide plates of different crack geometry (a/b and a/t) may produce entirely different types of yielding, and significantly different functional relations between the COD and the nominal strain ξ may result, such that the experimentally calibrated curve $\phi - \varepsilon/\varepsilon_0$ may locate above or below the Burdekin's design curve (see Fig. 4 and 3). Some criticism and confusion on the safety of the Burdekin design curve had thus been raised. Recent analysis and experiments (Soete and Denys, 1976; Soete, 1977; Tsai, 1976, 1977; Tsai and coworkers, 1978) drew attention to the ligament yielding disturbance and the effect of strain hardening. The conclusion is that the Wells' or Burdekin's formulas or design curves are valid only in the case of small cracks within large high strain zone without any interference of ligament yielding. However, since high strain concentration zone in actual engineering components is often encompassed fully by surrounding elastic region (contained plasticity), ligament yielding is impossible to develop for edge cracks and side surface cracks. Further, the deep surface crack is usually treated as a through the thickness crack of the same length. In all these actual engineering cases, the Burdekin's design curve seems consistent with the results of experimental calibration under the absence of ligament yielding disturbance and the results of extrapolation of F.E. calculations. Finally, it is important to note that, while the above analytical and experimental calibration results are in good agreement with the COD design curve, the comparison of the predictions with the results of large-scale fracture tests shows that the critical crack size at fracture is about 2-3 times larger than maximum allowable crack size estimated by the design curve based on initiation COD, owing to the presence of stable crack growth after initiation.

Recent works on J -integral design curve and formulas for high strain brittle fracture analysis have been proposed by various authors (Begley and coworkers, 1974; Tsai, 1976; Merkle, 1976; Turner, 1978). The results show essential equivalence of the two approaches. However, owing to the complexity and limited accuracy, no experimental calibration of J -integral under general yielding condition had been conducted to study the effects of the crack geometry, the ligament yielding disturbance, the stress state, the presence of yielding plateau and the strain hardening parameter n of the materials.

CRACK GROWTH WITHIN CYCLIC STRAIN ZONE

Crack growth rate and life analysis under strain fatigue condition is another important topic of high strain fracture analysis. It can be described by COD or J -integral parameters. The formulation using J -integral is most simple and has been proposed by Tsai (1976) and independently by Mowbray (1976) for fully reversed strain cycling. However, since J -integral is based on the deformation theory of plasticity and can be applied only under monotonic loading condition, its application to crack growth analysis under fully reversed strain fatigue condition needs some elucidation. In fully reversed strain controlled fatigue experiment, each unloading stage of a cycle is followed by reversed compressive plastic deformation, during which all the residual stress and strain field of the crack body will be removed, after unloading of the compression, the crack body is free again from any stress field except some strain hardening or softening of the material. Thus during the unloading of the next cycle that makes the crack to open and grow, the crack body is monotonically loaded again from its free state and the J -integral does determine the crack tip field and control the magnitude of crack advance $\Delta a = da/dN$.

Based on the identity of crack tip field under the equality of $\Delta K^2/E'$ for small scale yielding to the J -integral for general yielding, i.e. $\Delta K^2/E' = J$, we may suppose equal crack growth rate in these two cases. Thus $(da/dN)_{G.Y.} = (da/dN)_{S.S.Y.} = A\Delta K^n$, substituting $\Delta K^2/E' = J$ into the later formula, we may have the following expression

$$(da/dN)_{G.Y.} = A(E'J)^{n/2} = CJ^r \quad (20)$$

for crack growth rate of a small crack within a large cyclic strain zone with $r = n/2$ and $C = A(E')^{n/2}$. Substituting (19) into (20) we have

$$da/dN = C(2\pi qa \int \sigma d\varepsilon)^r \quad (21)$$

where $J = 2\pi qa \int \sigma d\varepsilon$ and $\int \sigma d\varepsilon$ are corresponding maximum J -integral value and maximum work density absorbed by the material during the unloading stage of the cycle that makes the crack to open and propa-

gate. By integrating the eq. (21) from initial crack depth a_i to final crack depth a_f , and assuming $\int \sigma d\epsilon$ to keep constant, we arrive at the following fatigue life formula

$$N_f (\int \sigma d\epsilon)^r = (a_f^{1-r} - a_i^{1-r}) / C(r-1)(2\pi q)^r \quad (22)$$

In order to test the applicability of the above analysis, LCF experiments of superalloy smooth specimens and precracked specimens with small initial cracks of two given depth ($a_i=0.22\text{mm}$ and $a_i=0.67\text{mm}$) had been conducted under controlled total strain range (Shen and Tsai, 1980), the result (Fig. 5) confirms the formula (22) with $r=1.8$ and $C=3.03$ and $a_f=2\text{mm}$ when the J -integral is in MN/m or MJ/m^2 and the crack length in mm. It is interesting to show that the value of $r=1.8$ and $C=3.03$ obtained from LCF life data of precracked specimens in Fig. 5 is in good agreement with the value of $r=n/2=1.8$ and $C=A(E/1-\nu^2)^{n/2}=2.45$ calculated from crack propagation data measured under small scale yielding condition, $da/dN=4.48 \times 10^{-10} \Delta K^{3.6}$. For smooth specimens, the

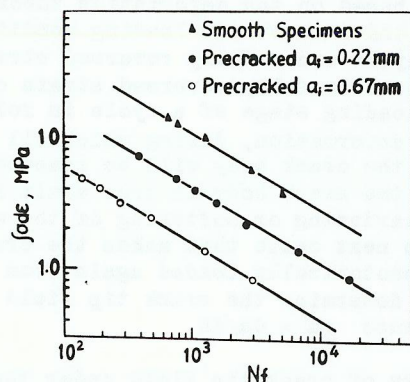


Fig. 5. Strain controlled LCF life of smooth specimens and precracked specimens with small pre-existing crack at room temperature for superalloy Ni-20%Cr-2.5%Ti-0.7%Al-1.5%Nb, aged at 750°C, 16 hr.

effective initial crack depth calculated from measured N_f , $\int \sigma d\epsilon$, $a_f=2\text{mm}$ and $r=1.8$, $C=3.03$ is $a_i=40\mu\text{m}$, which is a little smaller than the mean grain size ($70\mu\text{m}$) suggesting that a given number of cycles is required for the crack nucleation along the persistent slip band in the grain.

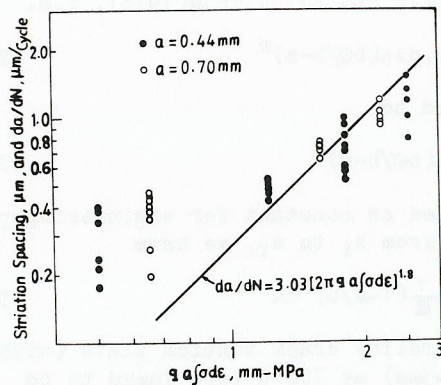
The advantage of the above fracture mechanical approach for predicting the high strain fatigue life is its ability to take into account the effect of small pre-existing flaws, while the conventional "local strain approach" based on Coffin-Manson relationship can be used only

when no pre-existing crack is present in the high strain region of the components. Thus, the present approach is most suitable for welded structure where the probability of small defects of 0.1-0.5mm in size is high within critically strained regions.

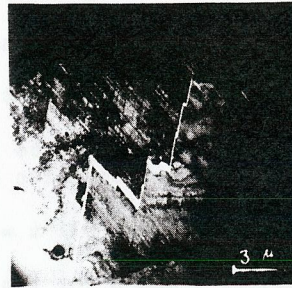
While the above LCF life prediction based on high strain fracture mechanical analysis shows some promise of engineering use, there are still problems on its practical applications. Firstly, it is apparent from Fig. 5, that the life of the precracked specimens with initial crack depth $a_i=0.22\text{mm}$ under strain fatigue condition is only 20-30% of the life for smooth specimens. Thus, as the engineering crack formation life is usually defined as the life of forming a small crack of $1/32"$ (0.8mm) in length or 0.2-0.3mm in depth, the crack propagation life which can be described unambiguously by the above analysis is only a minor part of the whole life. Although the engineering crack formation stage is actually a stage of crack propagation of very small crack (10 μm to 0.2mm) within area of high cyclic strain, the applicability of the above fracture mechanical analysis is doubtful since the strength of the crack tip field is rather low due to the negligible size of the crack, and the gross stress-strain range will have a larger contribution to the cumulative damage of the material. In this case, the crack initiation and early growth rate should be controlled by overall stress-strain range rather than by the crack tip field parameter J .

Finally, in fracture mechanics and the continuum model of fatigue crack propagation it is usually assumed that plastic strain ahead of crack tip is microscopically homogeneous and that each loading cycle produces a fatigue striation spacing. However, comparison of the fatigue striation spacing with the crack growth rate calculated by equation (21) using experimentally determined value of $r=1.8$ and $C=3.03$ shows that at small crack and low growth rate stage with $da/dN \leq 0.2 \mu\text{m}/\text{cycle}$, the striation spacings are apparently larger than the growth rate da/dN (Fig. 6a) and have a lower limit (about 0.1-0.2 μm) for the superalloy. This means that at early stage of crack growth each strain cycle does not necessarily produce a striation at the whole crack front, but some redundant cycle may be required before sufficient damage accumulates to cause a crack extension step in each grain. Furthermore, TEM observation of thin foils cut from the fatigued superalloy smooth specimen shows that the plastic strain is microscopically inhomogeneous and concentrated at discrete slip bands (Fig. 6b). The crack forms and propagates only along the intense slip bands. This means that the fatigue striation spacing can only be the multiple of the slip band spacing. For the superalloy studied, the smallest slip band spacing is about 500 \AA and equals approximately the size of the γ' phase. Thus, the fatigue striation spacing should not be smaller than $2 \times 500\text{\AA} = 1000\text{\AA}$. This is consistent with the above SEM measured result. Thus, the above TEM and SEM observations show that the assumptions on the microscopic homogeneity of plastic strain and the one to

one correspondence of loading cycle and fatigue striation in fracture mechanics is no longer true in early stage of crack growth, and the physical meaning of the above result of high strain fracture analysis and experiment needs further interpretation.



(a)



(b)

Fig. 6. Comparison of fatigue crack growth rate da/dN and the fatigue striation spacing (a), and transmission electron micrograph showing the crack path along intense slip band (b).

CRACK GROWTH WITHIN CREEP STRAIN ZONE

In high temperature zone of engine components small pre-existing cracks may sometimes be present or form by hot corrosion and their interaction with grain boundary cavitations under high temperature creep condition can be deleterious which causes the small pre-existing crack to grow rapidly. Most experiments on creep crack growth were conducted using specimens with long crack under ligament creeping condition or under creep bending condition as in DCB specimen, however, most cracks in high temperature components are rather small in comparison with section size of the components, be it formed by welding or by hot corrosion, furthermore, fixed term inspection and service repair do not allow the small cracks to grow large, so that from the view point of life design and fracture control it is urgent need to conduct experiment and analysis on crack growth and stress rupture life of precracked superalloy specimens or components with small pre-existing cracks where general creeping condition prevails. Our experiment on stress-rupture life of engine disk superalloy (Ni-20%Cr-2.5%Ti-0.7%Al-1.5%Nb) specimens shows that small pre-existing crack seriously reduces the stress rupture life and strength of the superalloy (Fig. 7).

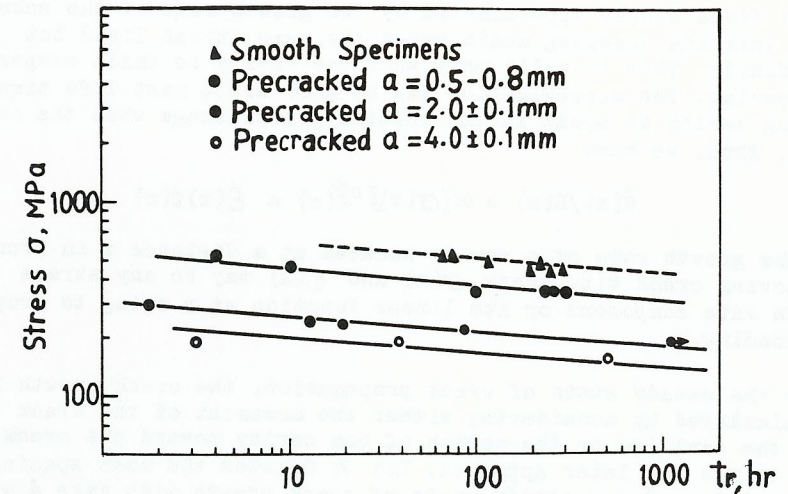


Fig. 7. Stress rupture life of smooth and precracked superalloy specimens at 700°C .

Inspection of the fracture surface shows that the crack grows along grain boundaries by growth and coalescence of cavities in front of the crack border. Thus, micromechanical analysis of creep crack growth rate based on cavity growth by power law creep ($\dot{\epsilon} = \alpha \sigma^n$) within the crack tip field and coalescence with the main crack along grain boundaries should be performed in order to establish the crack growth law under creep condition. The derivation is similar to that given by Nix (1977), but here the COD rate and creep J-integral parameter \dot{J} are used instead of stress intensity factor K, since for small crack within general creeping zone under high stress and temperature, the creep strain rate is rather high such that the elastic crack tip field will be relaxed soon after loading and the crack tip field should be controlled by the constitutive equations of power law creep.

For power law creeping materials with $\dot{\epsilon} = \alpha \sigma^n$ the constitutive equations and its solutions are similar to those of pure power hardening materials except that the strain and displacement components ϵ_{ij} and u_i should be replaced by corresponding rate quantities $\dot{\epsilon}_{ij}$ and \dot{u}_i . For a spherical cavity of instantaneous radius R in an infinite media of power law creeping material, its radial displacement rate \dot{R} can be expressed as

$$\dot{R}/R = \alpha \sigma^n R(n) \quad (23)$$

This expression can easily be obtained by using a similar dimensional analysis in deriving equation (5) for pure power hardening materials. Suppose that the growth rate of a spherical cavity in the crack tip

stress field can be approximated by the growth rate of the same cavity in an infinite creeping media under the same stress field but acting at infinity. This is valid only when the cavity is small compared with its spacing. The approximation may be good since most life time of the growing cavity is spent in the initial growth stage when the cavity is small. Thus, we have

$$\dot{R}(x)/R(x) = \alpha[\sigma(x)]^n \hat{R}(n) = \dot{\epsilon}(x)f(n) \quad (24)$$

for the growth rate of a cavity located at a distance x in front of the moving crack tip, where $\sigma(x)$ and $\dot{\epsilon}(x)$ may be any stress and strain rate component or its linear function at x owing to proportional loading.

Under the steady state of crack propagation, the crack growth rate can be calculated by considering either the movement of the crack tip toward the cavities or the motion of one cavity toward the crack tip. Here we use the later approach. Let λ denotes the mean spacing of the cavities. Under steady state of crack growth with rate $\dot{a} = da/dt$, each cavity, while approaching from a large distance $x = x_0$ to the crack tip region at $x = \lambda/2$, should grow from its initial radius R_0 to the final radius $R_f = \lambda/2$ and coalesces at the crack tip to ensure the steady crack growth. Thus, with $\dot{a} = da/dt = -dx/dt$ (since $a+x = \text{const.}$) and $dR(x) = \dot{R}(x)dt = -R(x)dx/\dot{a}$ in mind, from equation (24) we have

$$\int_{R_0}^{\lambda/2} \frac{dR(x)}{R(x)} = \int_{x_0}^{\lambda/2} f(n) \dot{\epsilon}(x) \left(-\frac{dx}{\dot{a}}\right)$$

and

$$\dot{a} = da/dt = \frac{f(n)}{\ln \lambda/2R_0} \int_{\lambda/2}^{x_0} \dot{\epsilon}(x) dx \quad (25)$$

Furthermore, for power law creeping materials, similar equations as (4) and (6) can be obtained from which we should have:

$$\dot{\epsilon}(x) = (\dot{\delta}/a)\varphi(x/a, n) \quad (26)$$

where $\dot{\epsilon}(x)$ may be any strain-rate component at x . Substituting the later expression into (25) we arrive at the following crack growth law described by crack opening displacement rate parameter $\dot{\delta}$.

$$da/dt = B\dot{\delta} \quad (27)$$

where $B = [f(n)/\ln(\lambda/2R_0)] \int_{\lambda/2}^{x_0/a} \varphi(x/a, n) d(x/a)$ can be measured by creep crack growth experiment. $\lambda/2a$

Similar crack growth law described by creep J-integral parameter \dot{J} can also be obtained by substituting the HRR singularity relationship $\dot{\epsilon}(x) = \alpha(J/\alpha I_{n,x})^{n/n+1} \hat{\epsilon}(0, n)$ into the equation (25), i.e.

$$da/dt = C\dot{J}^{n/n+1} \quad (28)$$

Using the plane stress F.E. results of $\dot{\delta}$ for crack tension plate of power law creep material given by Shih and Hutchinson(1976), i.e.

$$\dot{\delta} = \alpha g_2(a/b, n) a (b\sigma/b-a)^n \quad (29)$$

the equation (27) can be transformed to

$$da/dt = Da(b\sigma/b-a)^n \quad (30)$$

where $D = \alpha B g_2(a/b, n)$ can be treated as constant for engineering purpose. By integrating equation (30) from a_1 to a_f , we have

$$D \sigma^n t = \int_{a_1}^{a_f} \frac{1}{a} (1-a/b)^n da \quad (31)$$

The parameters n and D for the superalloy crack tension plate (with plate width $b=20\text{mm}$ and thickness $t=3\text{mm}$) at 700°C were found to be $n=10$ and $D=0.7 \times 10^{-26}$ to fit the experimental results shown in Fig. 7. The two lower solid lines are plots of equation (31) with $n=10$, $D=0.7 \times 10^{-26}$ and $a_f=10\text{mm}$. Although the above experimental result on thin plate under ligament creeping condition can be extrapolated to $a/b \rightarrow 0$ to obtain the crack growth law of a small crack in a large general creeping thin plate $a = a_1 \exp[0.70 \times 10^{-26} \sigma^{10} t]$, however, in most engine components, small surface cracks are usually met, where the plane strain condition and general creeping case prevail against plane stress and ligament creeping. Thus, we have conducted stress rupture experiment on tension round bar of 10mm in diameter with small pre-existing surface crack of depth $0.5\text{--}0.8\text{mm}$ under plane strain condition. It is difficult to analyse the crack growth rate and life of a surface crack in a tension round bar under ligament creeping condition owing to the geometrical complexity, and we must confine the experiment to the general creeping condition, that is, the stress rupture experiments of the tension bar with small surface crack of $0.5\text{--}0.8\text{mm}$ depth were interrupted so that the final crack depth a_f would not be larger than 2.5mm . Under this general creeping condition, from equation (8) we have $\dot{\delta} = 2\pi q a (\alpha \sigma^n)$, substituting into (27) and integrating, we obtain

$$D \sigma^n t = \ln(a_f/a_1) \quad (32)$$

where $D = 2\pi q \alpha B$. Using the data of interruption experiments, the parameters D and n for the superalloy at 700°C under plane strain condition were determined to be $n=10$ and $D=1.02 \times 10^{-28}$, and the crack growth formula under plane strain and general creeping condition is given by $a = a_1 \exp[1.02 \times 10^{-28} \sigma^{10} t]$. It is interesting to note that the crack growth rate for the superalloy under plane strain condition is about two order lower than under plane stress condition. SEM exa-

mination of the fracture surface shows that the cavity size and spacing at the mid section of the plane strain specimen is apparently smaller than that of plane stress specimen. This may relate to the lower creep strain rate at the crack tip and so lower cavity growth velocity under plane strain condition, such that more cavities can nucleate before their coalescence. The above experimental result shows that small surface crack under plane strain and general creeping condition may behave differently in comparison with through crack in thin plate under plane stress and ligament creeping condition. Thus, in order to predict accurately the crack growth rate and life of engine components with pre-existing small surface crack, experiment and analysis on crack growth and stress rupture life of specimens with small pre-existing surface crack under plane strain and general creeping condition is needed.

CONCLUSION

High strain fracture analysis is an important topic for engineering materials and structures. It includes the analysis of crack formation and crack growth of small cracks within the area of high monotonic, cyclic or creep strain. While the formulations of high strain fracture problems using crack opening displacement parameters (δ or δ_j) and J-integral parameters (J or J) based on pure power hardening or power law creeping model are simple and show some promise for engineering applications, there are still problems remaining to be solved. In high strain brittle fractures, analysis of the stable crack growth and the instability point is an important topic for further study. Recent developments in J controlled stable crack growth and the concept of tearing modulus show some prospects for this analysis. Further, in high strain fatigue and creep fracture, the crack tip singularity strength is very low owing to the negligible crack depth at the crack formation or early crack growth stage, and the gross cyclic strain range or creep strain may have a larger contribution to the fatigue or creep damage in the bulk. Thus, it is thought that the crack formation life or early crack growth life should be controlled by gross strain rather than by crack tip field parameters. In these cases, micro-mechanism investigations and micro-mechanical analysis of the damage process and the early crack growth in combination with the above fracture mechanical analysis should give a better solution in prediction. However, TEM and SEM investigations show that the crack forms and propagates either along intense slip bands in strain fatigue (Fig. 6b), or along grain boundaries in creep fracture (Fig. 7b), where fatigue damage or creep damage (cavity growth) accumulates. This damage localization in the bulk caused by gross strain and its close interaction with the crack tip makes the materials more sensitive to the small crack tip field. Thus, it is believed that although the crack tip singularity field is low due to the small crack size, the crack tip field parameters may still control the crack growth rate and life and the above high strain fracture mechanical

analysis may still be approximately valid or can be modified to include the effect of the gross damage in the bulk, since the major contribution of the later is to accelerate the growth of the main crack.

REFERENCES

- Begley, J. A., J. D. Landers, and W. K. Wilson (1974). Fracture Analysis. ASTM STP 560. 155-169.
- Burderkin, F. M., and M. G. Dawes (1971). Practical use of linear elastic and yielding fracture mechanics with particular reference to pressure vessels. Conference on Practical Application of Fracture Mechanics to Pressure-Vessel Technology, Inst. Mech. Eng., London.
- Goldman, N. L., and J. W. Hutchinson (1975). Int. J. Solids Structures, 11, 575-591.
- Ilyushin, A. A. (1946). Prikladnaia Matematika i Mekhanika, 10, 347.
- Merkle, J. G. (1976). Int. J. Pressure Vessels and Piping, 4, 197-206.
- Nix, W. D., D. K. Matlock, and R. J. Dimelfi (1977). Acta Met., 25, 495-503.
- Sato, K., and M. Toyoda (1979). An engineering assessment of general yielding fracture based on strain criterion. IIW Colloquium on Practical Applications of Fracture Mechanics to the Prevention of Failure of Welded Structures. B6, 110-120.
- Shih, C. F., and J. W. Hutchinson (1976). J. Eng. Mater. & Technol., 98, 289-295.
- Soete, W., and R. Denys (1976). Acceptability of defects in plate loaded beyond general yield. IIW Doc. X-837-76, Sydney.
- Soete, W. (1977). Fracture, Vol. 1, 775-804. ICF4, Waterloo.
- Tsai, C. K. (1976). Acta Metallurgica Sinica, 12, 45-67.
- Tsai, C. K. (1977). Acta Metallurgica Sinica, 13, 246-262.
- Tsai, C. K., L. K. Lo, H. H. Chen, P. H. Cheng, C. C. Lu, and P. C. Chang (1978). Crack opening displacement analysis in areas of high nominal strain. IIW Doc. X-900-78, also in Chinese J. Mech. Eng., 15, 39-51.
- Turner, C. E. (1978). An analysis of the fracture implications of some elastic plastic finite element studies. Proc. 1st Int. Conf. on Numerical Methods in Fracture Mechanics, Swansea.
- Wells, A. A. (1963). Brit. Weld. J., 10, 563.